Supporting Information for "Modeling global vegetation gross primary productivity, transpiration and hyperspectral canopy radiative transfer simultaneously using a next generation land surface model—CliMA Land"

Contents of this file

1. Figures S1
2. Note S1

Introduction

Figure S1 plots the comparison of soil water time series from ERA5 reanalysis data and flux tower observations at AU-Tum (site h of Figure 2 in the main text).

Note S1 describes the method we used to invert hyperspectral soil albedo from known broadband PAR and NIR albedo values.

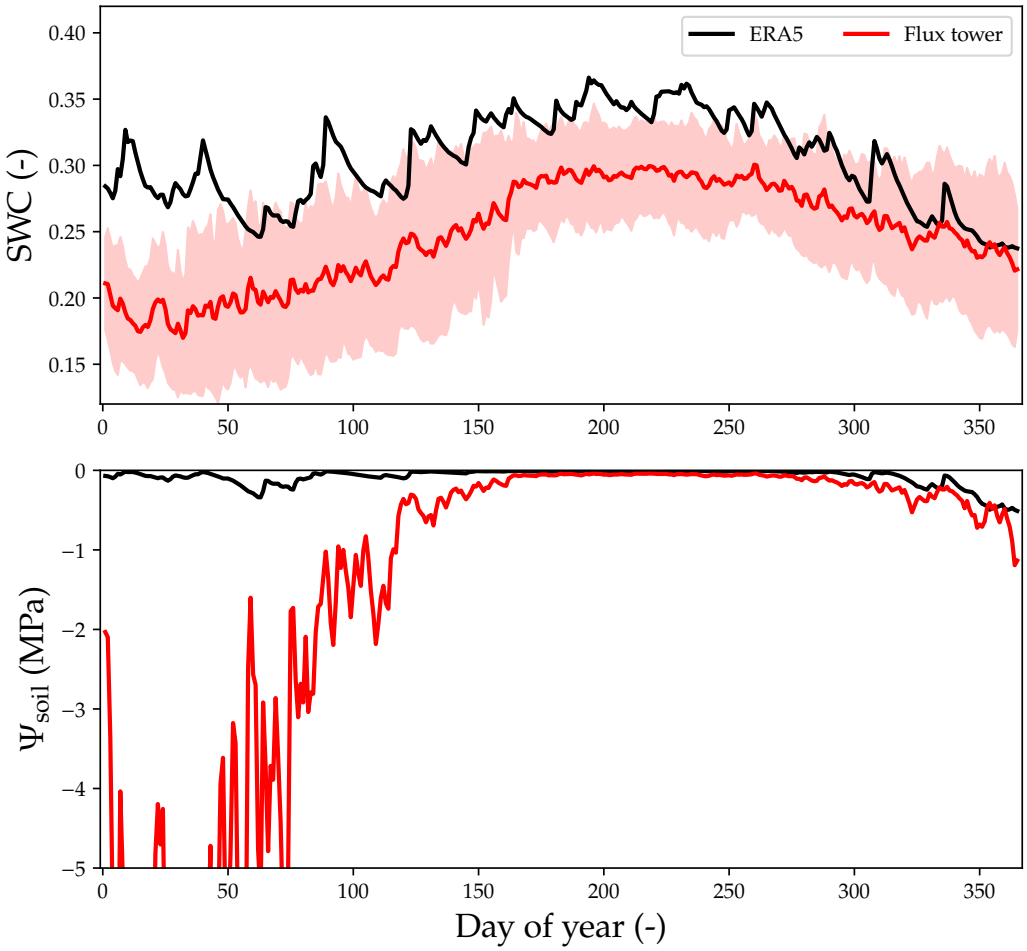

Figure S1. Comparison of soil water time series from ERA5 reanalysis data and flux tower observations at AU-Tum (site h of Figure 2 in the main text). Soil water content (SWC) from ERA5 is averaged from that of four soil layers (black curve), and SWC from flux tower is averaged from that of the same day from year 2001 to 2014 (shaded red region indicates the standard deviation, SD). Soil water potential (Ψ_{soil}) is computed from corresponding SWC using the van Genuchten equation (van Genuchten, 1980) using the gridded soil hydraulic parameters from Dai et al. (2019) for the site. Red region plots the Ψ_{soil} with SWC in the range of mean ± SD.

Note S1. Hyperspectral soil albedo

Firstly, to derive hyperspectral soil albedo (400–2500 nm), we calculate soil albedo values at photosynthetically active radiation (PAR) region (400–700 nm) and near infrared (NIR) region (700–2500 nm), denoted as α_{PAR} and α_{NIR} respectively, by linearly interpolating the reference values at completely wet and dry soils:

$$\alpha_{\text{PAR}} = \alpha_{\text{PAR,wet}} \cdot \text{RSWC} + \alpha_{\text{PAR,dry}} \cdot (1 - \text{RSWC}), \quad (1)$$

$$\alpha_{\text{NIR}} = \alpha_{\text{NIR,wet}} \cdot \text{RSWC} + \alpha_{\text{NIR,dry}} \cdot (1 - \text{RSWC}), \quad (2)$$

where RSWC is the relative volumetric soil water content (0 when completely dry, 1 when soil water content is saturated), the subscript "wet" denotes saturated soil, and the subscript "dry" denotes completely dry soil. The four reference albedo values at a RSWC = 0 and RSWC = 1 can be found in Community Land Model (Table S1).

Table S1. Reference broadband soil albedo.

Soil color	$\alpha_{\text{PAR,dry}}$	$\alpha_{\text{NIR,dry}}$	$\alpha_{\text{PAR,wet}}$	$\alpha_{\text{NIR,wet}}$
1	0.36	0.61	0.25	0.50
2	0.34	0.57	0.23	0.46
3	0.32	0.53	0.21	0.42
4	0.31	0.51	0.20	0.40
5	0.30	0.49	0.19	0.38
6	0.29	0.48	0.18	0.36
7	0.28	0.45	0.17	0.34
8	0.27	0.43	0.16	0.32
9	0.26	0.41	0.15	0.30
10	0.25	0.39	0.14	0.28
11	0.24	0.37	0.13	0.26
12	0.23	0.35	0.12	0.24
13	0.22	0.33	0.11	0.22
14	0.20	0.31	0.10	0.20
15	0.18	0.29	0.09	0.18
16	0.16	0.27	0.08	0.16
17	0.14	0.25	0.07	0.14
18	0.12	0.23	0.06	0.12
19	0.10	0.21	0.05	0.10
20	0.08	0.16	0.04	0.08

Our adapted method differs from the original CLM approach, which uses

$$\alpha_{\mathrm{PAR}} = \max(\alpha_{\mathrm{PAR,dry}}, \alpha_{\mathrm{PAR,wet}} + 0.11 - 0.4 \cdot \mathrm{SWC}),$$

$$\alpha_{\mathrm{NIR}} = \max(\alpha_{\mathrm{NIR,dry}}, \alpha_{\mathrm{NIR,wet}} + 0.11 - 0.4 \cdot \mathrm{SWC}),$$

where SWC is the absolute volumetric soil water content (0 when completely dry, < 1 when saturated). Our adapted soil albedo method better matches experimental observations than the original CLM approach (Figure S2).

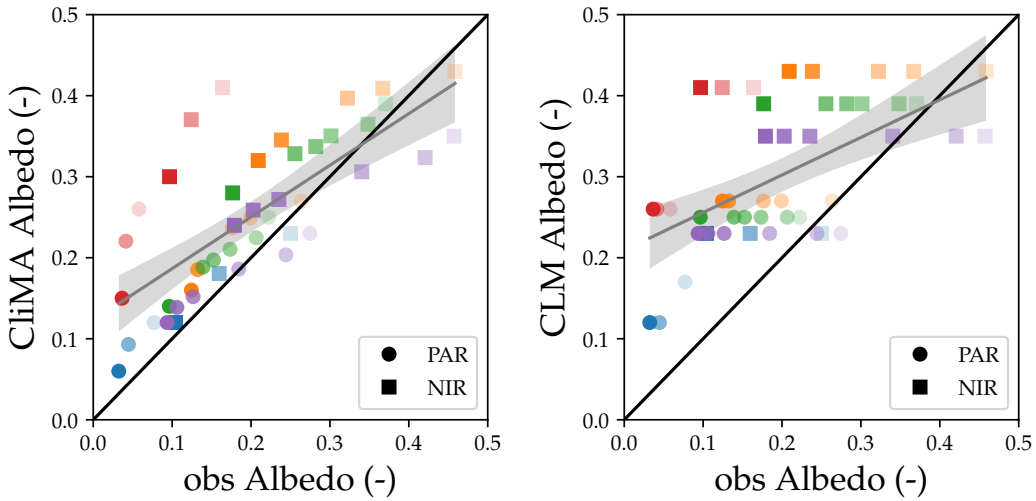

Figure S2. Comparison of the broadband albedo computed using the CliMA Land and CLM approach. Data from (Jiang & Fang, 2019).

Secondly, we expand the broadband albedo values to hyperspectral by weighing the characteristic soil albedo bands (three soil spectral vectors derived from dry soil database, and one moisture spectral vector derived from wet soil database):

$$\alpha(\lambda) = \sum_i f(i) \cdot A(i, \lambda), \tag{3}$$

where $\alpha(\lambda)$ is the albedo at wavelength λ, $f(i)$ is the weight of the ith characteristic albedo band, and $A(i, \lambda)$ is the ith characteristic albedo band. See Figure S3 for the four bands.

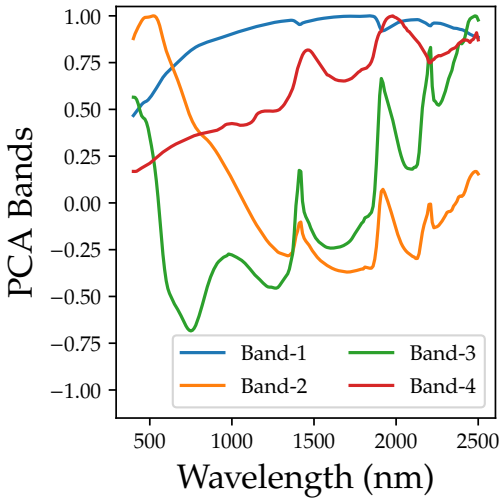

Figure S3. Characteristic soil albedo bands of the GSV model (Jiang & Fang, 2019). Band 1–3 are soil spectral vectors derived from dry soil database, and band 4 is spectral vector derived from wet soil database.

We use six methods to fit the weights: three methods using only first two characteristic bands (two fitted weights) and three methods using all four characteristic bands (four fitted weighted). Each of the categories contains (1) point method that fits averages, (2) curve method that fit curves, and (3) hybrid method that fits a point and a curve. The six methods are labeled as 2P, 2C, 2H, 4P, 4C, and 4H, respectively. The point method weighs the PAR and NIR region equally, and minimizes the sum of the square error between the averages:

$$\min \left[\left(\overline{\alpha_{\mathrm{PAR,mod}}} - \alpha_{\mathrm{PAR,ref}} \right)^2 + \left(\overline{\alpha_{\mathrm{NIR,mod}}} - \alpha_{\mathrm{NIR,ref}} \right)^2 \right]. \tag{4}$$

The curve method assumes the target is a two-piece flat curve that the PAR region is constant at $\alpha_{\mathrm{PAR,ref}}$ and the NIR region is constant at $\alpha_{\mathrm{NIR,ref}}$, and minimizes the square error between modeled and target curves:

$$\min \overline{\left(\alpha_{\mathrm{mod}} - \alpha_{\mathrm{ref}} \right)^2}. \tag{5}$$

The hybrid method weighs the PAR and NIR regions equally, and minimizes the sum of (1) the square error between the averages in the PAR region and (2) square of mean absolute difference between modeled and target curve in the NIR region:

$$\min \left[\left(\overline{\alpha_{\mathrm{PAR,mod}}} - \alpha_{\mathrm{PAR,ref}} \right)^2 + \left(\overline{|\alpha_{\mathrm{NIR,mod}} - \alpha_{\mathrm{NIR,ref}}|} \right)^2 \right]. \tag{6}$$

See Figure S4 for the examples of the fitting methods. Overall, 4H performs the best (Figure S5), and we use it in our CliMA Land simulations. Note here that method 4P fits 4 values from 2 albedo so that it does not converge. As a result, method 4P has extremely high error compared to others.

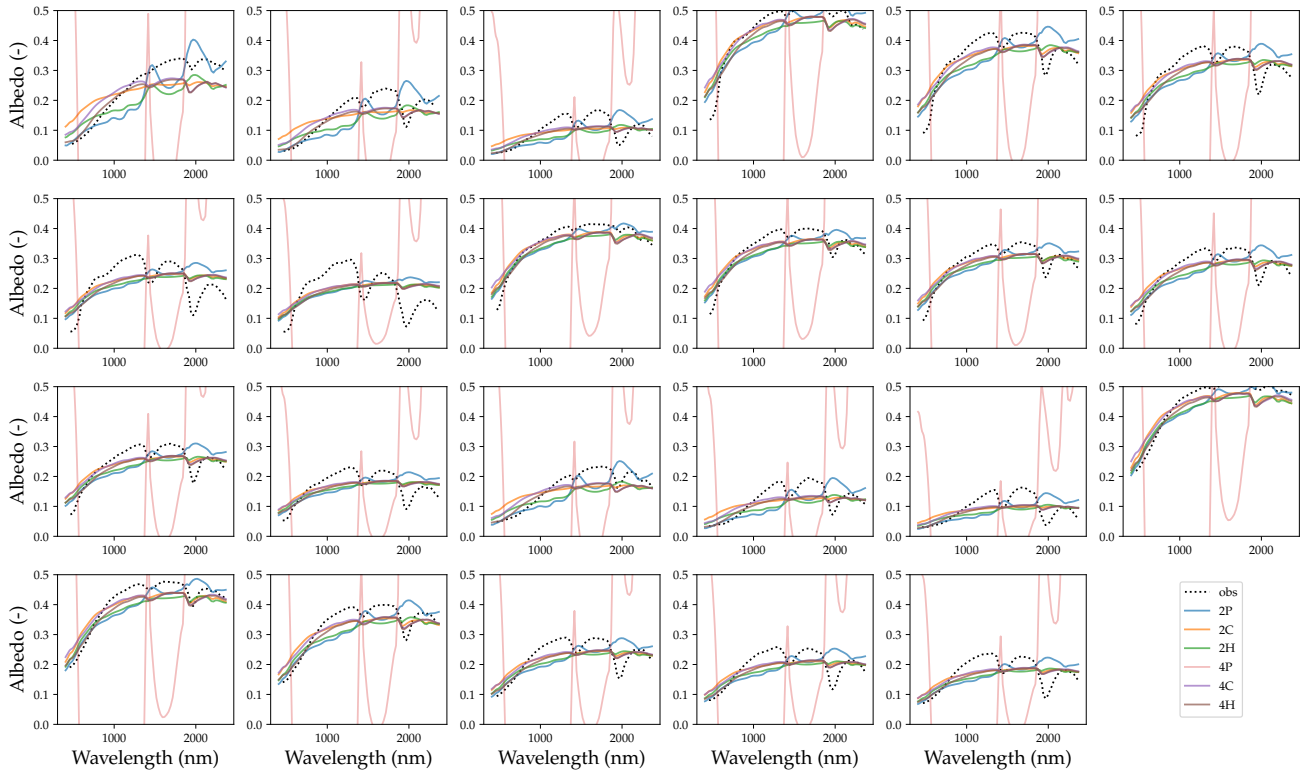

Figure S4. Examples of the performances of the six fitting methods. The 23 spectral curves and soil moisture data are from Jiang and Fang (2019).

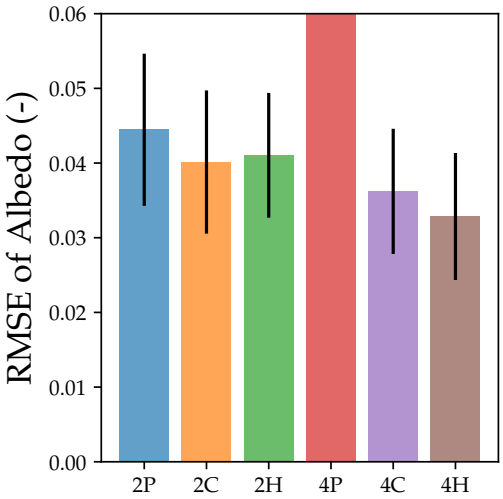

Figure S5. Performances of the six fitting methods. The 23 spectral curves and soil moisture data are from Jiang and Fang (2019).

References

Dai, Y., Xin, Q., Wei, N., Zhang, Y., Shangguan, W., Yuan, H., ... Lu, X. (2019). A global high-resolution data set of soil hydraulic and thermal properties for land surface modeling. *Journal of Advances in Modeling Earth Systems*, *11*(9), 2996–3023.

Jiang, C., & Fang, H. (2019). Gsv: a general model for hyperspectral soil reflectance simulation. *International Journal of Applied Earth Observation and Geoinformation*, *83*, 101932.

van Genuchten, M. T. (1980). A closed-form equation for predicting the hydraulic conductivity of unsaturated soils. *Soil science society of America journal*, *44*(5), 892–898.